Geophys. J. Int. (1998) **134,** 663–676

Anomalous surface waves associated with deep earthquakes, generated at an ocean ridge

M. Furumura,* B. L. N. Kennett and T. Furumura†

Research School of Earth Sciences, Australian National University, Canberra ACT 0200, *Australia*

Accepted 1998 March 3. Received 1998 February 26; in original form 1997 September 23

SUMMARY

Broad-band seismograms observed at regional distances from deep earthquakes display large-amplitude Rayleigh and Love waves with a predominant period of about 20 s, although deep earthquakes in laterally homogeneous structures do not generate such surface waves. Since the propagation direction of the surface waves inferred from particle motion is approximately radial and the group velocity of the surface waves observed at each station is similar, it can be assumed that the surface waves have travelled close to the great-circle paths. Back projection allows us to determine the region in which these surface waves are generated. Many of the zones from which the surface waves appear to originate are located close to the Norfolk Ridge, where crustal structure has strong lateral heterogeneity. This suggests that the surface waves are generated by the interaction of body waves from the deep earthquakes with this strongly heterogeneous crustal structure.

In order to investigate the effect of such heterogeneity in crustal structure on seismic wavefields, we have modelled the P–SV wavefield using a pseudospectral method. The results show that surface waves such as those observed can be generated by ridge structures and indicate that sedimentary layer thickness plays a very important role. We suggest that such unexpected surface waves from deep earthquakes may prove useful for delineating heterogeneity in shallow structure.

Key words: continental margin, deep earthquakes, Lord Howe Rise, Norfolk Ridge, surface waves, synthetic seismograms.

1 INTRODUCTION

From May 1993 to October 1996, the SKIPPY Project (Van der Hilst *et al.* 1994) operated a sequence of arrays of portable broad-band seismic recorders on the Australian continent, with the principal objective of delineating 3-D structure in the crust and upper mantle beneath the continent. In the broad-band records of SKIPPY stations in eastern Australia we found unexpected wave trains with the characteristics of surface waves associated with deep earthquakes occurring at nearby subduction zones. The surface waves with large amplitude are seen after SS or sS, and are characterized by a predominant period of about 20 s.

Although large-amplitude surface waves of relatively short period are a characteristic feature of the seismograms for shallow events, they are not expected for a laterally homogeneous structure for events deeper than 200 km. The character of the observed surface-wave trains suggests a shallow level of generation, so the origin of these surface waves would appear to lie in the interaction of seismic waves from the deep events with the complex crustal structure between Australia and the subduction zones.

The Melanesian Borderland, the area bounded to the west by Australia and to the east by New Zealand and the Tonga–Kermadec trench (see Fig. 1), includes some inactive marginal basins, formed during the process of seafloor spreading between 60 and 80 Ma (Jongsma & Mutter 1978). Many studies of the crustal structure of this area, such as the velocity structure (e.g. Shor, Kirk & Menard 1971) and magnetic anomalies (e.g. Hayes & Ringis 1973), have revealed that the Melanesian Borderland comprises two large continental blocks with thick sediments associated with deep crustal roots embedded in oceanic material. The continental margin near 150°E also shows strong heterogeneity; the seafloor slope is quite steep, especially at the eastern margin of the Australian continent. These heterogeneous crustal structures may be related to the generation of the anomalous surface waves.

* Present address: Hokkaido University, Kita-ku, N10W8, Sapporo 060, Japan. E-mail: mitsuko@apgeo.sci.hokudai.ac.jp

† Present address: Hokkaido University of Education, Midorigaoka 2-34-1, Iwamizawa 068, Japan.

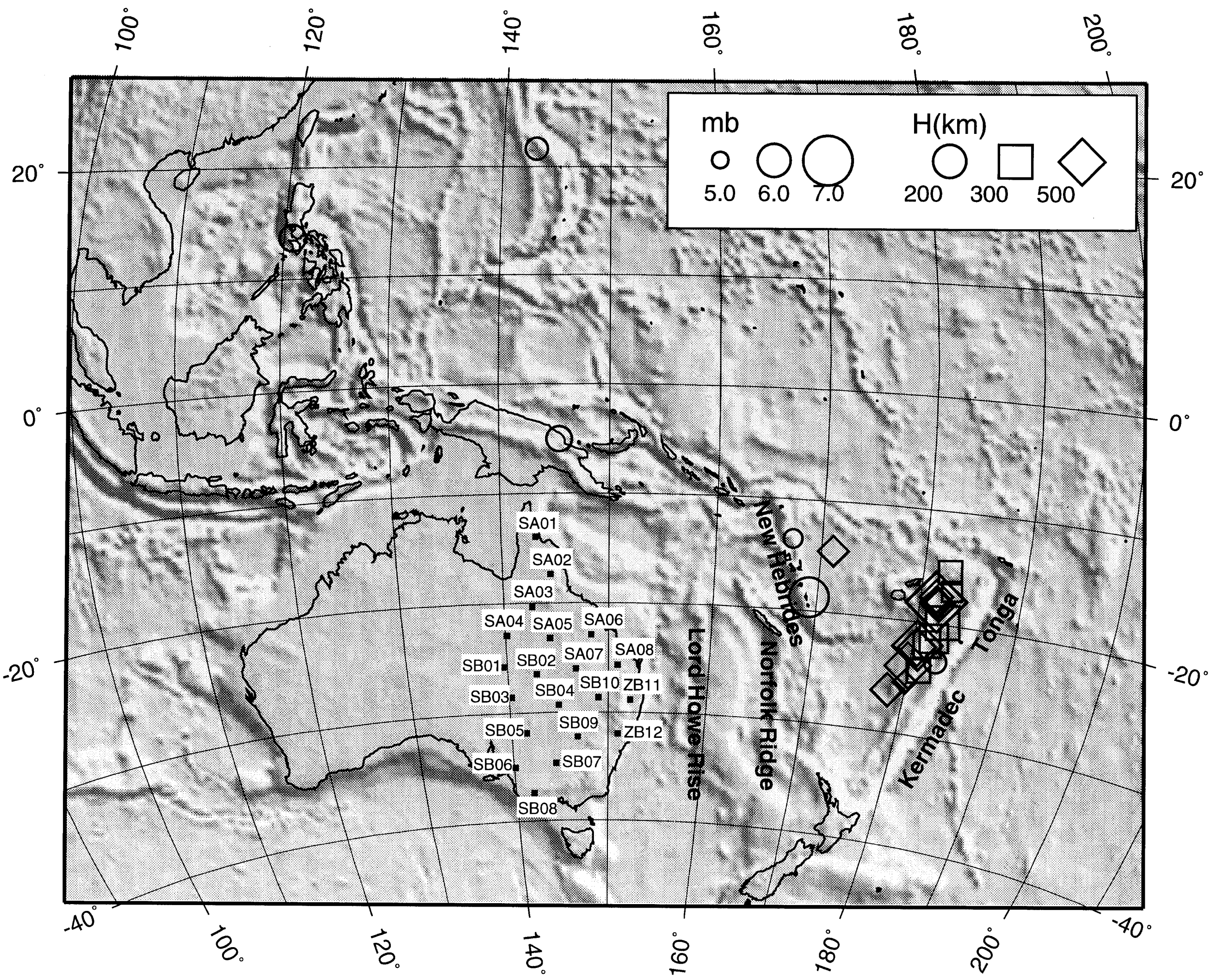

Figure 1. 23 deep earthquakes used in this study. Circles, squares and diamonds indicate earthquakes with depths of 200 to 300, 300 to 500 and more than 500 km, respectively; the symbol size is related to body-wave magnitude. A relief image of topography over mainland Australia and the adjacent ocean is also shown. The SKIPPY arrays are indicated by solid squares.

In this study we investigate the origin of the 20 s phases and the relation of these phases to heterogeneous crustal structure in the Melanesian Borderland. First, we determine the wave types of the unexpected surface waves by examining their group velocities and particle motions. Then, we use the arrival times of the phases to locate possible zones of generation for the 20 s surface waves and to elucidate their relation to known heterogeneous crustal structures. Finally, the excitation of surface waves from deep earthquakes and their subsequent propagation are investigated by 2-D numerical modelling using the pseudospectral method for P–SV waves. The wavefield calculations complement the observations in the understanding of the excitation mechanism of the 20 s surface waves. From a set of numerical models for the anomalous surface waves, we can make inferences about the crustal structure.

2 SURFACE WAVES OBSERVED IN AUSTRALIA FROM DEEP EARTHQUAKES

The first two phases of the SKIPPY Project emplaced arrays of broad-band instruments in Queensland (SA01–SA08) from May to October 1993, and in southeastern Australia (New South Wales, Victoria; SB01–SB10, ZB11, ZB12) from October 1993 to April 1994 (Fig. 1). Each site was equipped with a Reftek 72A-07DAT recorder (24-bit resolution) and Güralp CMG-3ESP seismometers (flat response to ground velocity from 0.03 to 30 s). The sampling rate was 25 samples per second with GPS timing.

An examination of the records of deep earthquakes from the Tonga–Kermadec, New Hebrides and other subduction zones revealed a number of clear observations of surface waves with a dominant period of about 20 s, even though such waves would not be expected from the focal depth of the event in spherically symmetric earth models.

In order to investigate these surface waves, we selected records from deep earthquakes with a focal depth greater than 200 km to avoid contamination of the results by surface waves generated close to the sources. For these earthquakes, we can easily recognize the unexpected phases in the observed seismograms. Fig. 2 shows the original three-component velocity seismograms observed at station ZB11 for a deep earthquake which occurred beneath the Fiji Islands (1994 March 9, $H = 563$ km, $m_b = 6.6$). The arrival times of the body-wave phases are in very good agreement with theoretical

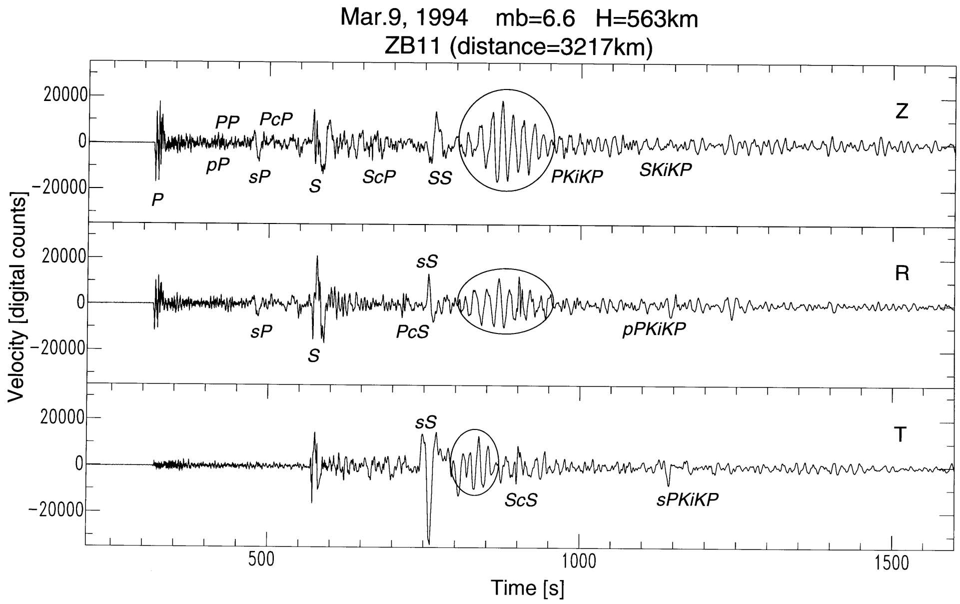

Figure 2. Original velocity seismograms of vertical (Z), radial (R) and transverse (T) components observed at station ZB11 for the Fiji Islands earthquake (1994 March 9, $H = 563$km, $m_b = 6.6$). Ellipses indicate the anomalous 20 s surface waves.

traveltimes calculated for the spherically symmetric IASP91 earth model (Kennett 1991). The unusual feature is the large-amplitude wave trains with a period around 20 s, at about 830 s on the transverse component and 870 s on the vertical and radial components. The amplitude of these arrivals is significant, almost as large as that of the *S* waves, but the arrival times do not correspond to any recognized seismic phases for the IASP91 model. We therefore seek an explanation in terms of heterogeneous structure.

The surface-wave characteristics of these unexpected phases can be seen in Fig. 3, in which we display filtered seismograms of the vertical component, and particle orbits for the waves in an interval of 45 s centred around 870 s after the origin time. The group velocities of the waves are shown for five frequency bands using Butterworth bandpass filters with cut-off frequencies between 0.035 Hz (28.6 s) and 0.085 Hz (11.8 s). The amplitude of the filtered seismograms is large in the frequency range between 0.05 Hz (20 s) and 0.071 Hz (14 s), and the wave train is clearly dispersed. The particle motion of the phases is retrograde in the vertical-radial plane with a predominant period of about 17 s, and the transverse component is very small. Thus, the phase observed at about 870 s can be recognized as being composed of Rayleigh waves. The earlier phase, near 830 s, which is dominant on the transverse component, can similarly be recognized as Love waves.

The 20 s surface-wave trains from this event are also observed at other stations, as shown in Fig. 4. Fig. 4(a) displays vertical-component seismograms for the same earthquake observed at 10 stations as a function of epicentral distance and time after the origin time. Rayleigh waves (indicated by bullets) are observed at most of the stations, with amplitudes similar to the *S* and *SS* phases. The arrival time increases with epicentral distance, with an apparent velocity of about 2.7 km s^{-1}, significantly slower than that of *S* and *SS*. The duration of the Rayleigh waves observed at ZB11 is about 100 s and phase dispersion extends the duration at greater epicentral distances. In Fig. 4(b) we show a record section of transverse-component seismograms of the same earthquake in which unexpected arrivals are observed at many stations. Since the apparent velocity of these phases (3.0 km s^{-1}) is slower than the *S* waves and faster than the Rayleigh waves, we can be confident that these later arrivals are Love waves. The amplitude of the Love waves is rather small, the duration of the phases is comparatively short and the dispersion is not as clearly developed as for the Rayleigh waves.

We have been able to identify such Rayleigh and Love waves with a predominant period of about 20 s for 23 out of 40 deep earthquakes between May 1993 and April 1994 (Fig. 1 and Table 1). The depths of these earthquakes range between 204 and 631 km, and most of them occurred at the Tonga–Kermadec trench. We seek a region where the anomalous surface waves could be generated from body waves by the influence of heterogeneous structure at shallow depth. In the Melanesian Borderland, there are ridges which are characterized by continental blocks embedded in oceanic material (Shor *et al.* 1971), implying significant heterogeneity in crustal structure in this oceanic region. A further heterogeneous region lies at the continental margin. To see which of these heterogeneous structures might generate the 20 s surface waves, we have estimated the likely generation points for these waves.

3 ORIGIN OF THE SURFACE WAVES

The points at which the 20 s surface waves are generated by conversion from body waves can be determined if we know the direction of travel and the group velocity, and if we can infer the wave type of the body-wave phases. The most reliable method of obtaining the direction of travel is array analysis, such as the frequency–wavenumber spectrum method or the semblance method, which also determines the phase velocity of the waves. However, we cannot apply those methods to the seismograms from the large-scale SKIPPY arrays because the predominant period of the surface waves is too short compared

Table 1. Deep earthquakes for which surface waves were observed in Australia. H is focal depth, mb is body-wave magnitude. The table lists the conversion points identified, group velocity (U), original body waves from which surface waves are converted (Type), epicentral distance of the conversion points (Point) and confidence of the conversion (C) for Rayleigh and Love waves.

Date (year/month/day)	Time (GMT)	Latitude (°N)	Longitude (°E)	H (km)	mb	Rayleigh waves U (km/s)	Type	Point (degree)	C	Love waves U (km/s)	Type	Point (degree)	C
1993/06/15	13:06	-4.99	145.46	227	5.5	2.6	S	3.0	A	3.2	S	1.0	A
1993/07/09	15:37	-19.78	-177.49	398	6.0	3.3	S	8.1	A	3.5	S	9.6	A
1993/07/23	16:38	-18.34	-178.10	631	5.4								
1993/08/05	12:42	-18.10	-178.33	616	5.4								
1993/08/07	17:53	-23.87	179.85	523	6.0	3.3	S	6.4	B	3.2	S	13.1	B
1993/08/20	11:52	21.69	143.06	288	5.3								
1993/08/21	09:42	-21.28	-178.02	427	5.7	3.2	S	11.2	B				
1993/09/16	06:51	-25.35	179.85	502	5.0								
1993/11/30	20:44	-17.00	-177.05	411	5.2								
1993/12/10	06:31	-22.18	-179.58	605	5.6	2.9	S	10.8	B	2.7	S	20.2	C
											sS	28.9	C
1993/12/24	05:18	-21.85	-178.65	445	5.6	2.8	S	19.1	C	3.0	S	13.9	B
							sS	25.3	C				
1994/01/19	16:26	-17.58	-178.50	533	5.4	2.7	S	15.7	A	3.3	S	14.6	A
1994/02/06	08:59	-13.59	167.19	204	5.1	2.6	S	3.4	B	3.5	S	5.6	B
1994/02/11	21:17	-18.77	169.17	206	6.4	2.8	S	6.0	A	3.3	S	5.0	A
1994/02/16	03:48	-26.27	178.27	606	5.4	2.6	S	9.2	B	2.6	S	12.3	B
1994/02/20	21:48	13.69	120.79	207	5.6	2.6	S	23.9	C	3.1	S	24.0	C
							sS	27.5	C		sS	28.0	C
1994/03/09	23:28	-18.04	-178.41	563	6.6	2.7	S	16.6	A	3.0	S	17.5	A
1994/03/10	12:25	-18.06	-178.26	600	5.2	3.1	S	10.4	B	2.8	S	18.5	C
											sS	27.5	C
1994/03/12	01:49	-14.50	171.09	612	5.3								
1994/03/20	01:20	-23.30	-177.49	213	5.3								
1994/03/31	22:40	-22.06	-179.53	580	6.1	3.0	S	13.3	B				
1994/04/01	17:16	-24.26	-178.98	378	5.4								
1994/04/02	15:34	-15.32	-177.50	395	5.4	2.8	S	17.5	C	3.0	S	18.4	C
							sS	22.7	C		sS	29.2	C

with the interstation distance of the array to provide a suitable estimate of the direction.

An alternative method is to infer the direction from the particle orbits of Rayleigh or Love waves. We applied polarization analysis (Vidale 1986) to obtain the dominant polarization direction of the surface waves. The inferred direction of travel for the surface waves lies within $\pm 10^\circ$ of the great circle for most of the earthquakes we analysed. However, polarization analysis does not work well when more than one phase is recorded simultaneously, and the deviation of the inferred direction of travel for the surface waves from the great-circle paths is not systematic. Hence, in this study we use great-circle paths as an approximation to the direction of travel for the anomalous surface waves. Furthermore, we take the group velocity from the record sections, making a particular choice for the wave type (P, S or sS) as the 'original body wave' which might generate the surface waves. We then draw a straight line as the traveltime curve of surface waves to obtain the epicentral distance at which the extrapolated traveltime of the surface waves matches the theoretical traveltime of the 'original body wave'. The theoretical body-wave traveltime is calculated using the IASP91 model. The estimated epicentral distance at which the surface wave would be generated from the 'original body wave' is then projected on to the ray path to each station.

In Fig. 5 the traveltime curve for a constant group velocity of 2.7 km s^{-1} is superimposed on the vertical-component seismograms observed for the Fiji event. We see that there are three possibilities for the generation of the Rayleigh waves:

(1) P-to-Rayleigh-wave conversion at an epicentral distance of $10.9 \pm 5^\circ$;
(2) S-to-Rayleigh-wave conversion at an epicentral distance of $16.6 \pm 5^\circ$;
(3) sS-to-Rayleigh-wave conversion at an epicentral distance of $23.4 \pm 3^\circ$.

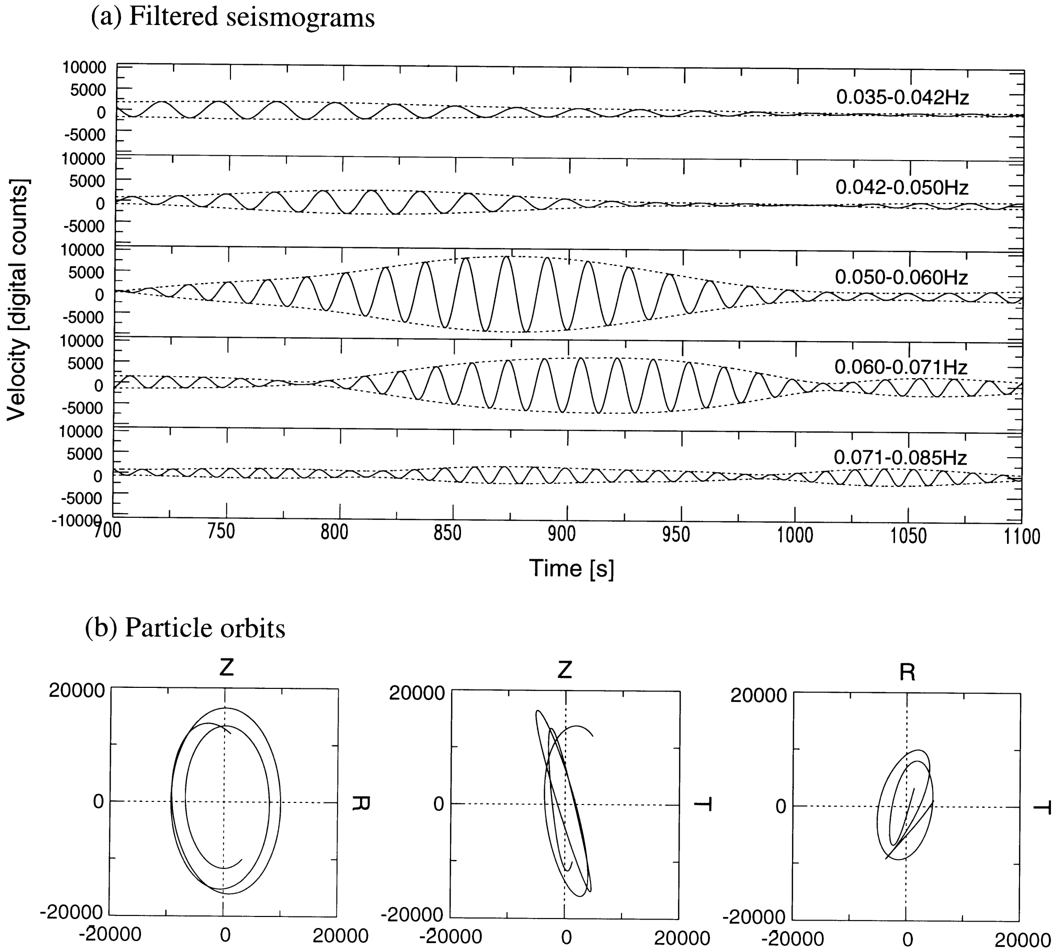

Figure 3. (a) Filtered seismograms of the vertical component of the event in Fig. 2 using five band-pass filters; the frequency range of each filter is shown above each trace. (b) Particle orbits from 855 to 900 s projected onto the vertical and two horizontal perpendicular planes, following filtering with a band-pass filter with cut-off frequencies of 0.04 and 0.077 Hz.

There are two S-wave branches with similar arrival times near the S-to-Rayleigh conversion points, so the S phases can carry significant energy to produce the observed Rayleigh waves. The corresponding conversion point between S body waves and Love waves (17.5°), deduced from the record section of the transverse-component seismograms, is very close to the S-to-Rayleigh-wave conversion point. Thus, it is probable that both the Rayleigh and Love waves are converted from S waves.

There are some deviations of the arrival times of the observed Rayleigh waves from a simple linear relation. The limits on acceptable group velocities are 2.6 to 3.2 km s^{-1}. This scatter in group velocity leads to a variation in the estimated conversion points of about 5°. The scatter may be caused by small differences in the crustal structure along the paths to each station.

Similarly, we estimated the likely generation points of Rayleigh and Love waves for each of the earthquakes by checking the possible areas of surface-wave generation for different classes of body waves. We have been able to estimate the slope of the arrival times for the surface waves for 15 of the 23 earthquakes. For the remaining events, the anomalous surface waves were observed at too few stations to determine the traveltime behaviour. The observed Rayleigh waves show group velocities between 2.6 and 3.3 km s^{-1}, with an average of 2.9 km s^{-1}, and the Love waves show group velocities between 2.6 and 3.5 km s^{-1}, with an average of 3.1 km s^{-1}. The major part of the Melanesian Borderland is characterized by continental-like crust, and the group velocity of the observed surface waves is in good agreement with theoretical values for a typical continent [the theoretical group velocity of the fundamental Rayleigh mode for the PEM-C earth model of Dziewonski, Hales & Lapwood (1975) changes from 2.8 to 3.5 km s^{-1} in the period range 25–13 s, and the fundamental Love mode has a group velocity close to 3.4 km s^{-1} in that period range].

We summarize the group velocity of the surface waves, the epicentral distance of conversion points from S and sS or SS (if the conversion point can be defined) and our confidence in the conversion process in Table 1. We regard a conversion process as having high confidence when the estimates of the two conversion points from the Rayleigh and Love observations lie close together (within 2°) and assign such cases to class A. Where it is difficult to define a conversion point for one wave type, we assign the case to class B, indicating a lower confidence of identification of the conversion process. Where we cannot judge which type of conversion process is more likely from the record sections alone, we assign the case

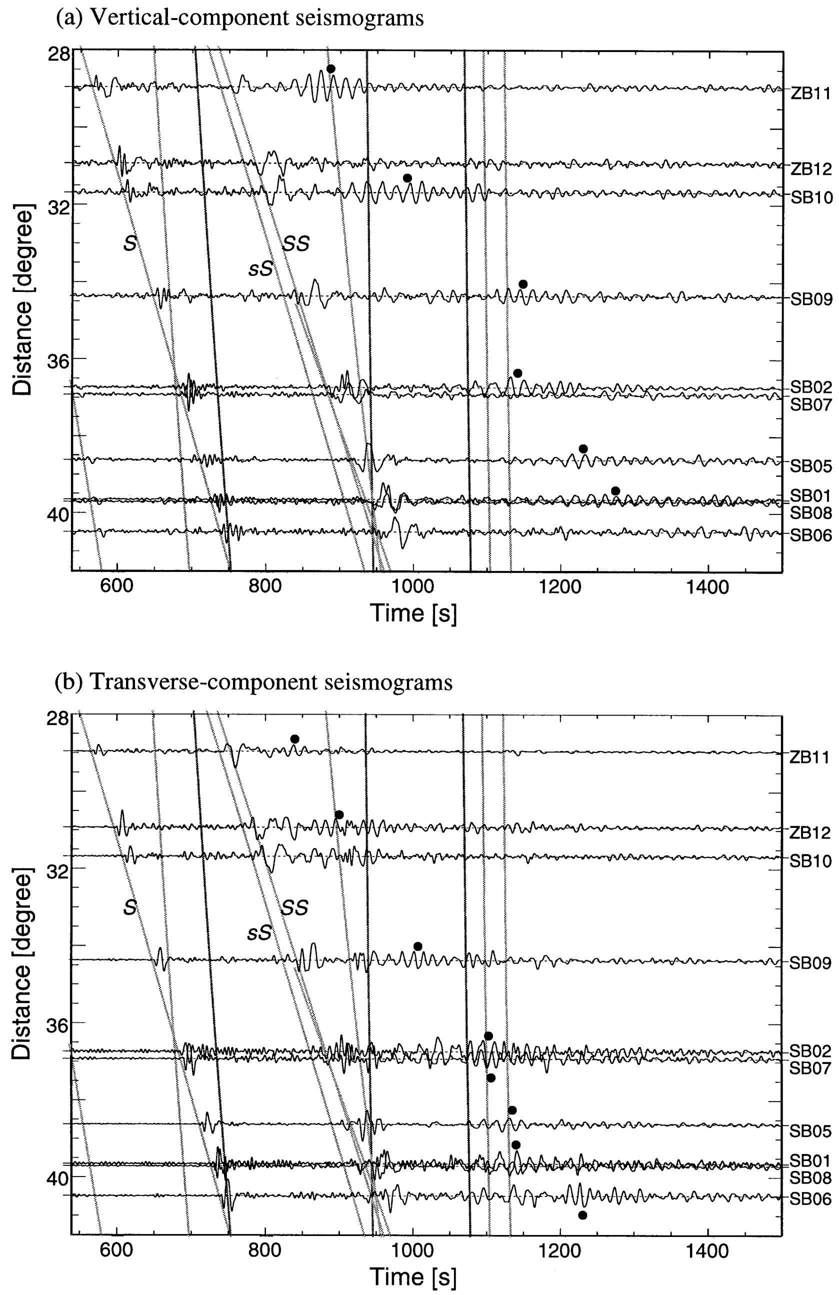

Figure 4. Velocity seismograms observed at 10 SKIPPY stations for the event in Fig. 2, for which large later phases (shown by bullets) can be discerned. Traveltime curves of body waves calculated for the IASP91 earth model are also plotted as thin lines. (a) Vertical components; (b) transverse components.

to class C. All conversion points classified as classes A and B arise for conversion from *S* waves.

From the information in Table 1, we can plot the conversion points on the great-circle paths. These points from the full set of stations are distributed in a band, because the SKIPPY arrays are very large, and so we may define the 'generation area' of the surface waves which encloses the conversion points on all great-circle paths for a single earthquake.

Fig. 6 displays the generation areas for the Rayleigh (a) and Love (b) waves corresponding to classes A, B and C. We have plotted a single generation area with a solid outline for events in class A, and with a dashed outline for class B events. Two possible generation areas are indicated by dotted outlines for events in class C, since we cannot judge which area is more probable. The generation area for both Rayleigh and Love waves corresponding to events in classes A and B is concentrated in the geographical region bounded by the 20°S and 32°S parallels and the 162°E and 170°E meridians for the earthquakes occurring at the New Hebrides and Tonga–Kermadec trenches. There is no significant difference in the location of the generation areas between the Rayleigh and the Love waves, which suggests that these two types of surface waves are generated by the same heterogeneous structure. The concentrated zone of generation areas is located very close to the Norfolk Ridge, one of the major heterogeneous structures in the Melanesian Borderland. In consequence, we conclude

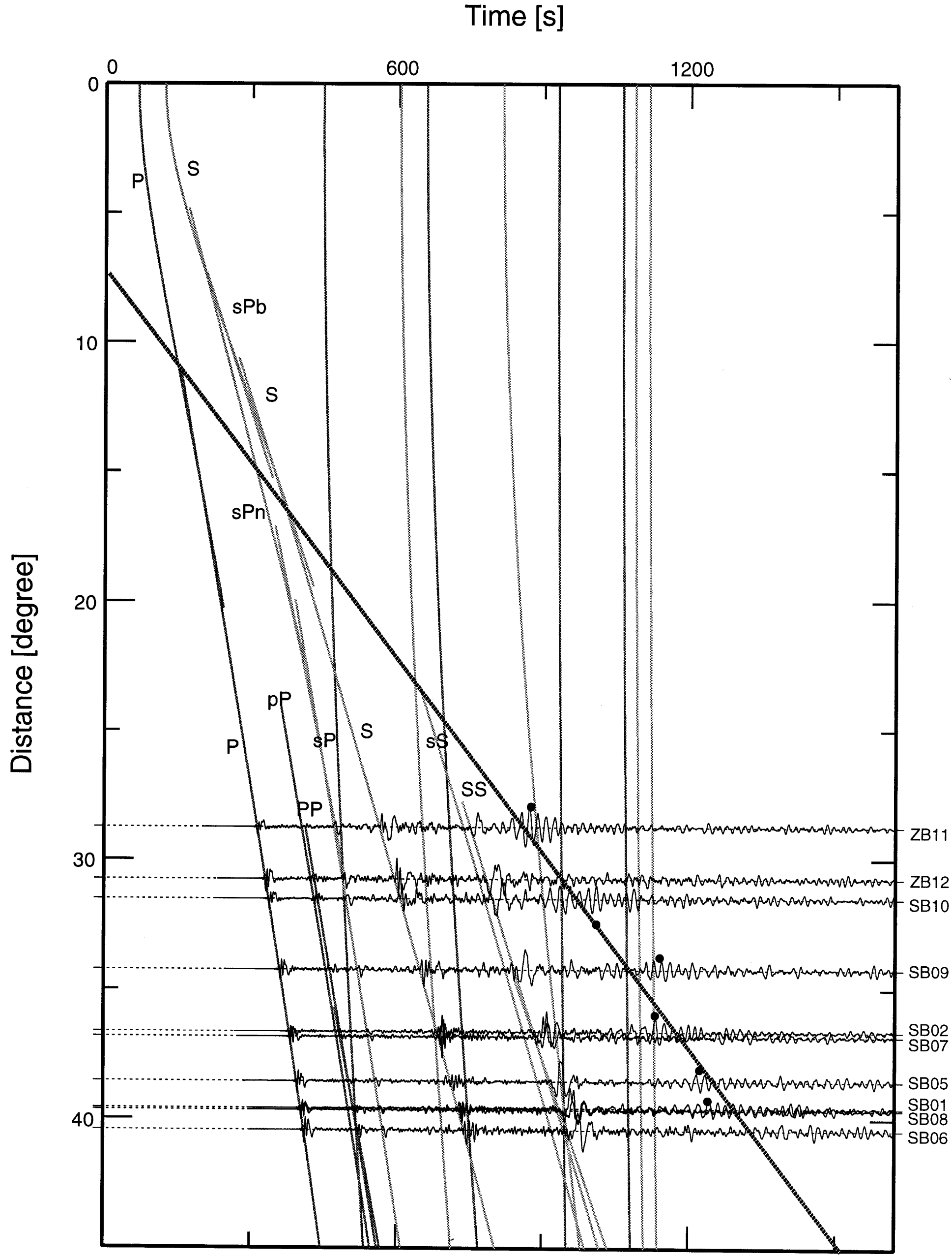

Figure 5. A traveltime curve for a constant group velocity of 2.7 km s^{-1} superimposed on the vertical-component seismograms in Fig. 4.

that surface waves associated with earthquakes beneath the Tonga–Kermadec trench are generated near the Norfolk Ridge.

There are some generation areas which are not related to the Norfolk Ridge, such as the easternmost section of the New Hebrides trench, where the direction of relative movement of the plate boundary reverses. In the case of earthquakes occurring to the north of Australia, the generation areas corresponding to *S*-to-surface-wave conversions are located at the northern continental margin. This may well arise because in the absence of oceanic ridges the most heterogeneous crustal structure encountered is at the continental margin.

For a few events, we cannot readily judge which phase might be the 'original body wave' giving rise to the surface waves. The probable generation areas are located near the Norfolk Ridge, on the Lord Howe Rise and very close to the continental margin, but we cannot discriminate amongst the possible points of origin.

4 NUMERICAL MODELLING OF SURFACE-WAVE GENERATION

In order to understand the generation of anomalous surface waves from deep earthquakes and to gain further insight into the relation between the heterogeneous structures and the surface waves, we have undertaken a series of simulations of the seismic wavefield with numerical modelling using the pseudospectral method (e.g. Furumura & Takenaka 1996; Furumura, Kennett & Takenaka 1998). We employed realistic geological structure models for the region and carried out the

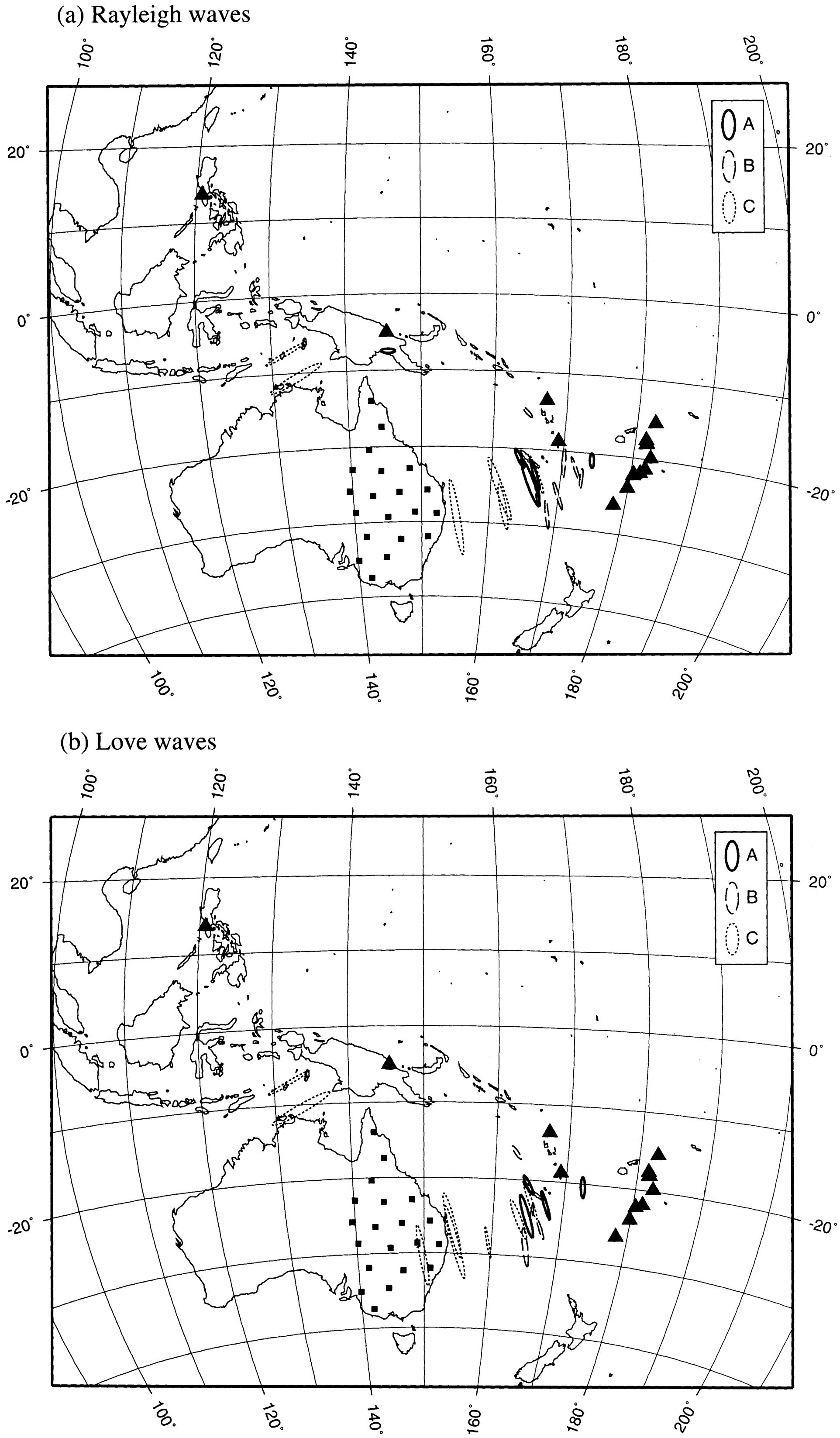

Figure 6. Generation area of the surface waves, classified into classes A, B and C (see Table 1). See Fig. 1 for the location of rises. (a) Rayleigh waves; (b) Love waves.

calculation using a 2-D elastic P–SV code to demonstrate the likelihood of surface-wave generation near the Norfolk Ridge.

The structure model used represents an E–W vertical cross-section through the Melanesian Borderland from the Tonga–Kermadec trench to the Australian continent, and is illustrated in Fig. 7. Following Shor *et al.* (1971), the Norfolk Ridge and the Lord Howe Rise are represented as continental regions in addition to the Australian continent; the remaining parts are treated as oceanic regions. Since the detailed structure is not known, the two styles of model are derived from the PEM-C and PEM-O earth models (Dziewonski *et al.* 1975), and are connected by a sinusoidally varying interface between layers and by linear interpolation of the velocities and density values within each layer. As the sedimentary thickness for the ridge region is not well determined, we have introduced a sedimentary layer of thickness 2 km for the ridge part of the model. The region of calculation covers a zone 3072 km long by 768 km deep and is represented using a grid of 1024 nodes horizontally by 256 nodes vertically with a uniform grid spacing of 3 km. A surrounding zone of 20 grid points was used as an absorbing buffer zone (Cerjan *et al.* 1985) to minimize the grid-edge effects.

In this complex model we placed a line source at 200 km depth below sea level, 440 km east of the top of the Norfolk Ridge, to simulate observed seismograms due to earthquakes occurring at the New Hebrides trench such as the earthquake on 1994 February 11 ($H=206$ km, $m_b=6.4$), for which the estimated region of generation for the anomalous surface waves lies 6° from the source. The source was a double-couple with a source time function of a pseudo-delta function with a width of 6 s. We present a sequence of snapshots of the seismic wavefield which have been separated into P and SV components by taking the divergence (P) and the curl (SV) of the radial and vertical displacements to identify the wave types. These components are displayed in light grey (P) and black (SV) to enhance S-wave visibility. We also display synthetic seismograms for ground velocity at a depth of 10.5 km in the crustal layer. The record sections are filtered using a low-pass filter with a cut-off frequency of 0.4 Hz to enhance the 20 s surface waves. The amplitude attenuation due to geometrical spreading is partially compensated by multiplying the seismograms by the corresponding epicentral distance.

Fig. 8 displays a sequence of detailed wavefield snapshots for the portion of the wavefield in a frame 900 km across by

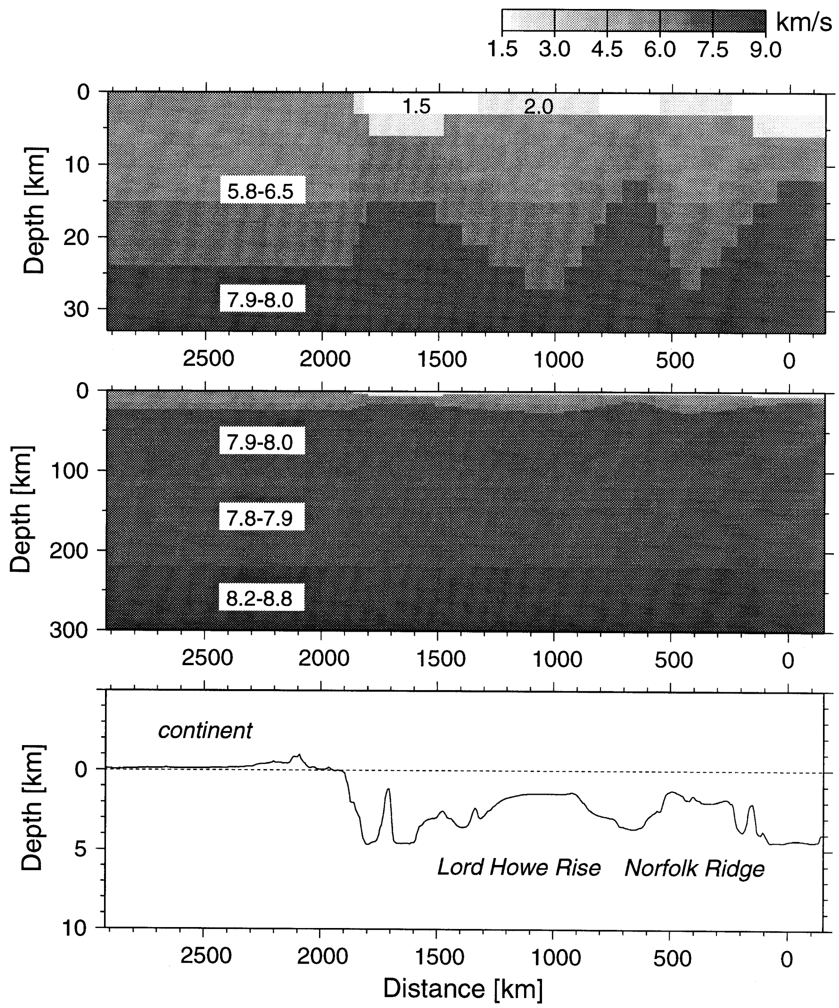

Figure 7. P-wave velocity structure model used for the calculation of the wavefield (top and middle panels), which has been constructed based on the topography along an E–W profile across the Melanesian Borderland (bottom panel). Numbers shown in the structure models indicate the P-wave velocity range in each layer. The broken line shown in the topography denotes sea level.

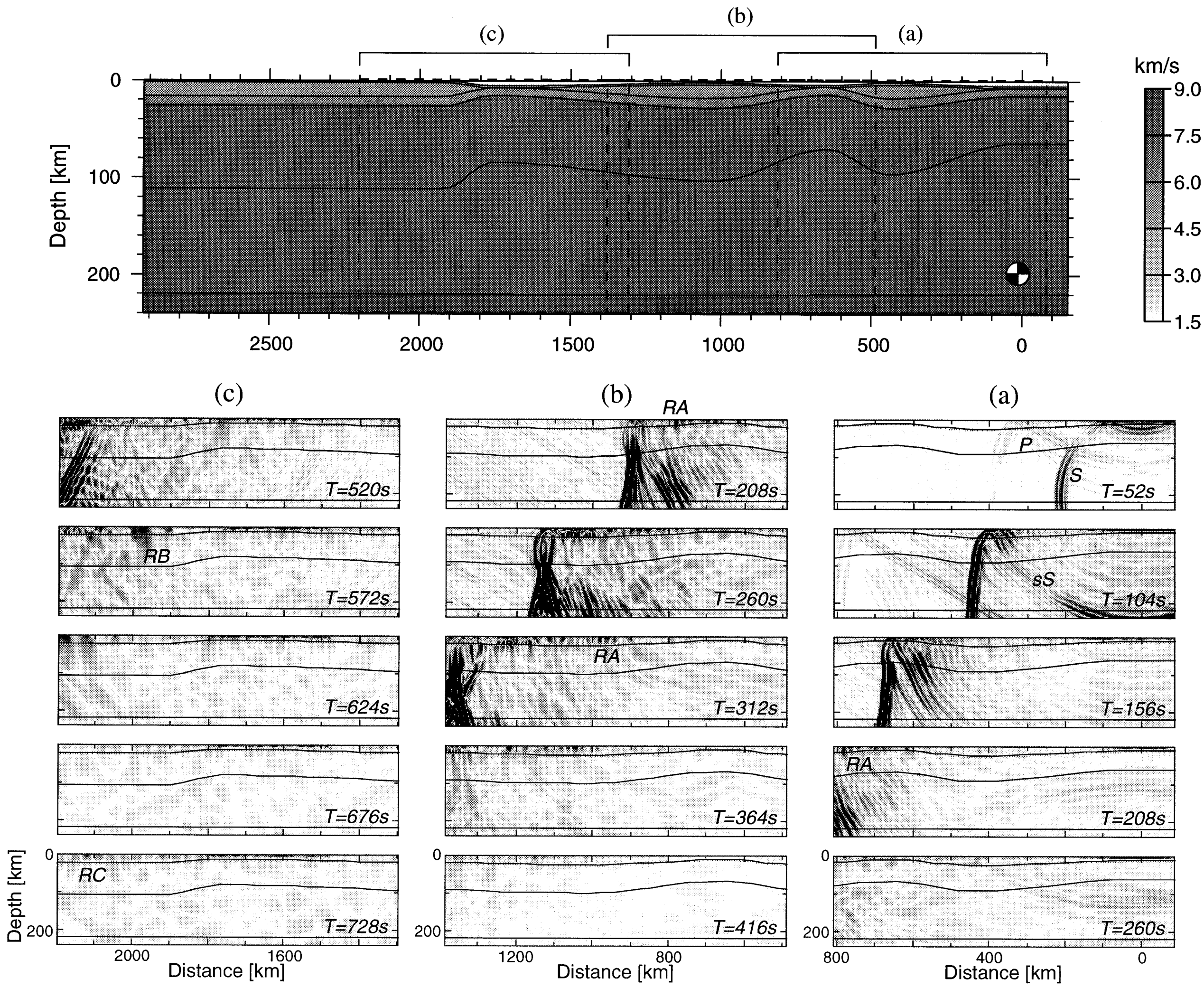

Figure 8. Snapshots of the seismic wavefield of the three regions, illustrating the P and SV components of the wavefield as a function of epicentral distance and time. The P-wave contribution is shown in light grey and the S-wave contribution in black. RA, RB and RC denote generated fundamental Rayleigh mode, and are linked with the symbols in Fig. 9. Velocity discontinuities are superimposed on snapshots as thin lines.

240 km deep with a 52 s interval between frames. In Fig. 8(a) this frame is set over the Norfolk Ridge for times from 52 to 260 s, in (b) around the Lord Howe Rise from 208 to 416 s and in (c) around the continental margin from 520 to 728 s. The amplitude of each frame is normalized so that the surface waves can be seen. In the top frame (52 s) of Fig. 8(a) we see the radiation of significant S energy from the dip-slip fault source upwards towards the surface, which produces *Sn* and *SmS* phases. These phases are multiply reflected at the Moho discontinuity and the ocean bottom as shown in the lower frames and build up a long coda after S waves. By 208 s (Figs 8a and b) the multiple S-wave reflections have produced Rayleigh waves (RA) at the 'valley' between the Norfolk Ridge and the Lord Howe Rise (the distance zone 700–1100 km away from the source) due to elevation of the Moho discontinuity. The Rayleigh waves have a large amplitude in the crust, are dispersed and propagate along the surface with a group velocity of 1.8 km s^{-1}. The predominant period is relatively short compared with observed anomalous surface waves. The waves are clearly seen on the east side of the Lord Howe Rise (the frames from 208 to 312 s of Fig. 8b), but the amplitude becomes small on the west side of the Lord Howe Rise, and almost disappears at the continental margin (Fig. 8c). Energy from the relatively short-period Rayleigh waves is transformed to longer-period waves at the continental margin, due to the change of crustal layer thickness, to produce Rayleigh waves with a predominant period of about 28 s (RB) and 17 s (RC), which are dominant in the continent in the frames from 572 to 728 s in Fig. 8(c).

4.1 Effect of sedimentary layers

In the preceding model, we simulated the generation of Rayleigh waves by the heterogeneous crustal structure at the ridge and its subsequent propagation into the Australian continent, but the amplitude was somewhat smaller than that of the observed Rayleigh waves on the continent. The most probable reason for the large difference in amplitude of the generated Rayleigh waves is heterogeneous structure at a shallow level along the ray path, because the shallow-level structure is strongly related to the generation and propagation of surface waves.

In order to examine the effect on different regional phases as the shallow level structure is varied, we built a second model in which the sedimentary layer was thickened by 4 km at the 'valley' and the peak of the Lord Howe Rise, and by 2 km at the continental margin. Fig. 9 compares the synthetic seismograms of the vertical and radial components for the two cases, which clearly shows the significant influence of the sedimentary layer thickness.

Fig. 9(a) displays the seismograms for the case of a fixed layer thickness of sediment (2 km), which is the same case displayed in Fig. 8. As in Fig. 8, we see the generation of relatively short-period Rayleigh waves (RA) at the 'valley' region, the disappearance of these Rayleigh waves at about 1100 km, and instead the appearance of two later phases (RB and RC) with longer period out to 1300 km in the synthetic seismograms. In addition, we can confirm the identification of the two later phases as Rayleigh waves, because the particle motion of both phases is retrograde at the surface and their amplitude decays as depth. The predominant periods of the phases RB and RC are about 28 and 17 s and the group velocities are about 3.5 and 3.2 km s^{-1}, respectively. From the comparison of the predominant period, group velocity and arrival time, the phase RC in the synthetic seismograms is more consistent with the observed Rayleigh waves in the continent than the phase RB, but its amplitude is rather small.

On the other hand, for the case of the sediment with varying layer thickness (Fig. 9b), large-amplitude Rayleigh waves are seen. Rayleigh waves (RA) are generated in the distance zone 700–1100 km from the source, as in the previous case. However, with a thick sedimentary layer at the 'valley' region, the amplitude of the Rayleigh waves is very large. The Rayleigh waves propagate across the distance zone from 800 to 1400 km with a group velocity of 3.5 km s^{-1}, and at 1400 km relatively long-period Rayleigh waves clearly appear in the synthetic seismograms, which correspond to RB and RC seen in the

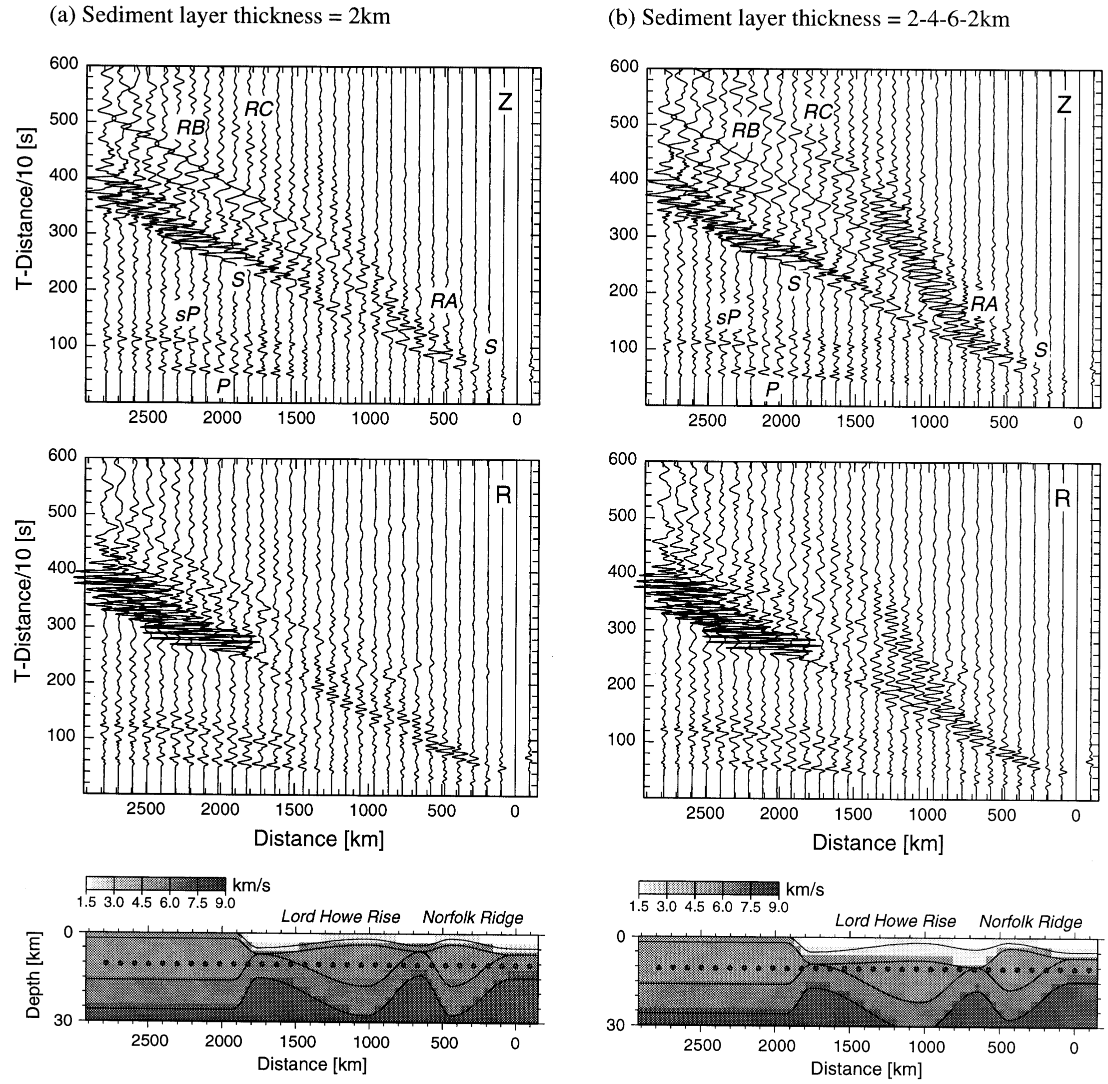

Figure 9. Synthetic velocity seismograms for vertical (Z) and radial (R) components at a depth of 10.5 km below sea level. Seismograms are filtered by a low-pass filter with a cut-off frequency of 0.4 Hz, multiplied by the epicentral distance of each station, and reduced by a velocity of 10 km s^{-1}. Station location is shown by circles in the velocity structures. (a) Fixed sedimentary layer thickness model; (b) varying sedimentary layer thickness model.

synthetic seismograms in Fig 9(a). The later Rayleigh wave, RC, has a large amplitude, almost comparable to the earlier one (RB). In order to confirm our model, we undertook simulations for several other structure models (the numerical results are not shown here), in which sedimentary thickness in the 'valley' region and on the Lord Howe Rise is thinner. However, the numerical results show weak generation of 20 s Rayleigh waves. This leads us to believe that the 20 s Rayleigh waves observed in the Australian continent may be generated by a ridge structure including a relatively thick sedimentary layer.

When we use the back-projection method for estimating generation area of the RB or RC Rayleigh waves, we find that the zone is relatively close to the epicentre, which is not fully consistent with the observations. This may be because we use velocity models for the simulation that are simpler than the real structure (see Zielhuis & Van der Hilst 1996), due to a lack of detailed information on the crustal structure in this area. We have modelled the crustal structure using two classes of the earth model PEM, which might explain the relation between unexpected surface waves and heterogeneous crustal structure, but there may actually be more complex perturbations of layer thickness and velocity and density in each layer. Heterogeneity of the crustal structure in the N–S direction, which is out-of-plane in the numerical models, may also exist. Some deviations of the arrival times and group velocities of the observed surface waves may also arise from the heterogeneous crustal structure.

4.2 Effect of source depth

We could observe 20 s surface waves at the SKIPPY stations for very deep earthquakes which have occurred at a depth of about 600 km along the Tonga–Kermadec trench such as the earthquake on 1994 March 9, for which the generation area of the anomalous surface waves lies about 17° away from the source. Since it is well known that the amplitude of the surface waves generated from a source diminishes as the depth of the source increases, we should verify the likelihood of surface-wave generation at the ridge region for such a very deep earthquake and examine source depth effects on the surface-wave generation. For this purpose, we constructed a further numerical model for a very deep earthquake occurring at the Tonga–Kermadec trench. A dip-slip fault source was placed at 600 km depth, 1250 km east of the peak of the Norfolk Ridge. In this case, calculation of the seismic wavefields within a region from an earthquake to the continent requires quite a large computer memory because of the deep source. We have shifted the region of calculation by 1010 km towards the east, and simulated the generation of the surface waves only at the ridge regions; we do not include the Australian continental margin. The velocity structure was the same as that used in Fig. 9(b), in which the sedimentary layer is very thick in the 'valley' region between the Norfolk Ridge and the Lord Howe Rise.

In this geographical setting, significant S-wave energy radiated from the very deep source propagates towards the Norfolk Ridge (the 120 s frame of Fig. 10b) and produces multiple S-wave reflections between the ocean bottom and the sediment–crust boundary or the Moho in the ridge (the 300 s frame of Fig. 10b). The multiple S-wave reflections in the crust generate a Rayleigh wave at the 'valley', where the sedimentary layer is quite thick (the 480 s frame of Fig. 10c). Since short-period waves scattered by the 'valley' tend to disappear in the Lord Howe Rise and the Rayleigh waves are dispersed, the Rayleigh waves with a predominant period of about 20 s (RA in Figs 10a and c) become much clearer in the wavefield by 800 s, though their amplitude is smaller than that for the relatively shallow earthquake. These Rayleigh waves will cross the continental margin (distance range 2800–2900 km) without any significant attenuation, because their predominant period is much longer than that of surface waves that are strongly affected by the continental margin.

5 DISCUSSION AND CONCLUSIONS

Anomalous Rayleigh and Love waves with a predominant period of about 20 s have been clearly observed in 23 deep earthquake seismograms recorded on the Australian continent. Likely zones of conversion from body waves to surface waves could be well determined for 15 earthquakes; many probable generation areas are clustered near the Norfolk Ridge and a few areas lie near the Lord Howe Rise or the continental margin. These are areas where the crustal structure shows large lateral variation. 2-D simulation of the seismic wavefield using the pseudospectral method for a P–SV elastic model has illustrated that the generation of surface waves from multiple S-wave reflections in the heterogeneous crust may occur at the ridge region and emphasize the significant effects of the sedimentary layer. This modelling study has confirmed the relation between the generation of anomalous surface waves and heterogeneous crustal structure. However, we do not yet have sufficient knowledge about the crustal structure to undertake any valid, direct comparison between synthetic seismograms and the observed records.

Continental margins are more commonly occurring heterogeneous structures than ridges. The influence of continental margins on the propagation of surface waves has been discussed by many researchers (e.g. Fitas & Mendes-Victor 1992), and it has been demonstrated that the margin tends to play the role of a low-pass filter for seismic waves propagating from the ocean towards the continent. In our simulation results, the continental margin did not have a major effect on propagation of the surface waves generated. This may arise from the relatively long period of these surface waves, so that the role of the continental margin may not be important. An additional effect may arise because our structure model is more complex than the previous studies, because of the close proximity of a continental rise to the continental margin. For earthquakes occurring north of the Australian continent, the influence of the continental margin on the seismic wavefield may be stronger because there are no ridge structures along the ray path. In these cases, surface waves can be generated from body-wave phases incident at the continental margin.

Modelling of the 20 s surface waves in the deep earthquake seismograms indicates the existence of very thick sedimentary layers in the region between the Norfolk Ridge and the continental margin in the Melanesian Borderland. The existence of a thick sedimentary layer in this region is consistent with McCracken (1979). Since the surface-wave generation is very sensitive to shallow-level structure, we may be able to use those surface waves to delineate heterogeneous structure, if we have sufficient observed seismograms along the ray paths to compare them with the synthetic seismograms.

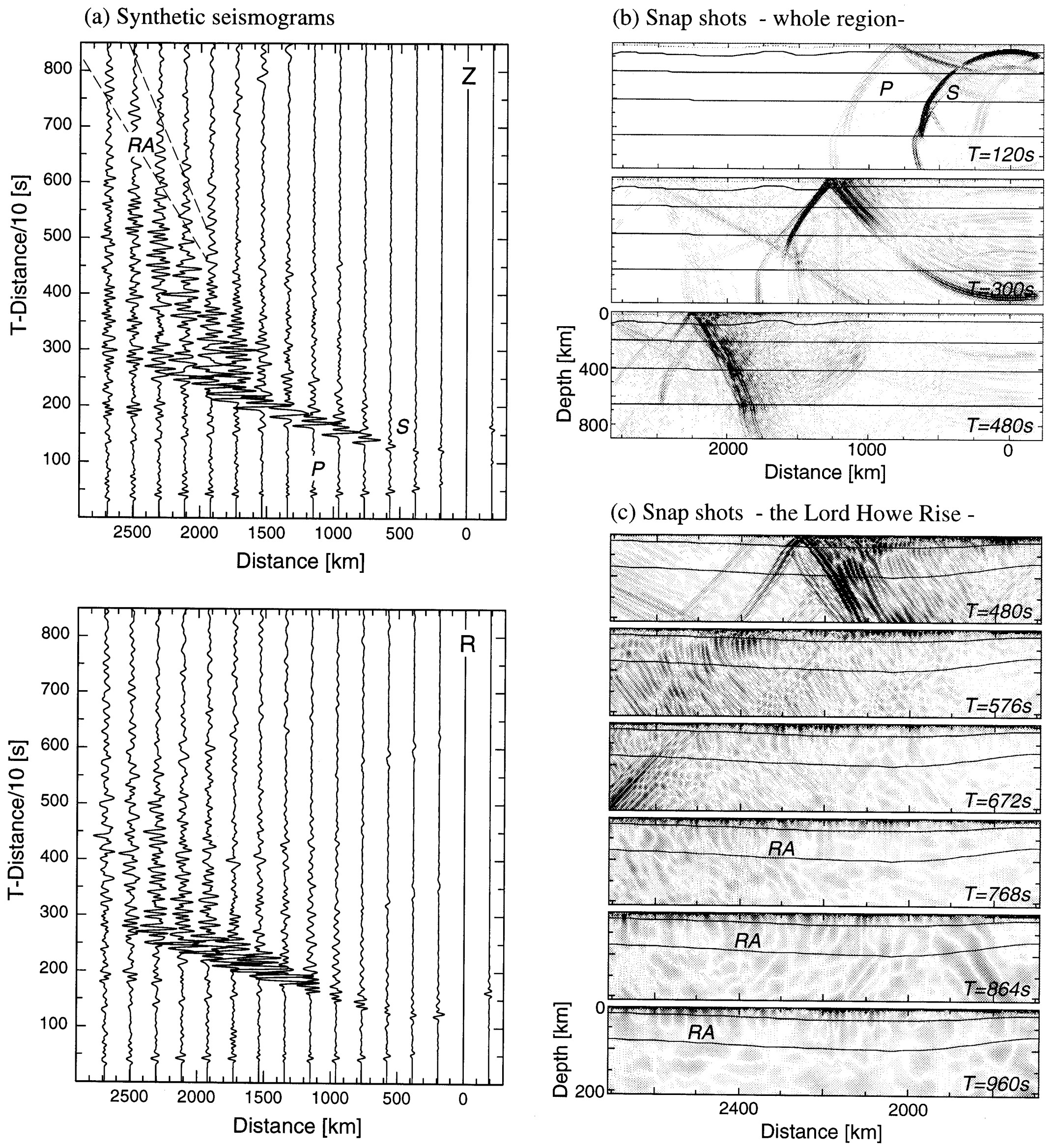

Figure 10. Synthetic velocity seismograms (a) and snapshots of the wavefield (b and c) for a deep dip-slip-type earthquake placed at 600 km depth. The seismograms at a depth of 10.5 km below the sea level are filtered by a low-pass filter with a cut-off frequency of 0.4 Hz, and snapshots of the seismic wavefield illustrate the P (light grey) and SV (black) contributions to the wavefield. Panel (c), 1023 km long by 420 km deep, focuses on the region of the Lord Howe Rise.

ACKNOWLEDGMENTS

The major part of this work was carried out in the Research School of Earth Sciences of the Australian National University during a visit in 1995 to the university by MF supported by a Visiting Fellowship. We thank the university and staff for their support. We also thank Dr Herb McQueen and Dr Jean Braun for their willing consent to the use of their topographic data. Constructive reviews by two anonymous reviewers and an editor are appreciated.

REFERENCES

Cerjan, C., Kosloff, D., Kosloff, R. & Reshef, M., 1985. A non-reflecting boundary condition for discrete acoustic and elastic wave equations, *Geophysics,* **50,** 705–708.

Dziewonski, A.M., Hales, A.L. & Lapwood, E.R., 1975. Parametrically simple earth models consistent with geophysical data, *Phys. Earth planet. Inter.,* **10,** 12–48.

Fitas, A.J.S. & Mendes-Victor, L.A., 1992. Rayleigh waves normally incident at a continental boundary, *Geophys. J. Int.,* **109,** 171–182.

Furumura, T. & Takenaka, H., 1996. 2.5-D modelling of elastic waves using the pseudospectral method, *Geophys. J. Int.,* **124,** 820–832.

Furumura, T., Kennett, B.L.N. & Takenaka, H., 1998. Parallel 3-D pseudospectral simulation of seismic wave propagation, *Geophysics,* **63,** 279–288.

Hayes, E.D. & Ringis, J., 1973. Seafloor spreading in the Tasman Sea, *Nature,* **243,** 454–458.

Jongsma, D. & Mutter, J.C., 1978. Non-axial breaching of a rift valley: evidence from the Lord Howe Rise and the southeastern Australian margin, *Earth planet. Sci. Lett.,* **39,** 226–234.

Kennett, B.L.N., 1991. *IASPEI 1991 Seismological Tables,* Research School of Earth Sciences, Australian National University, Canberra.

McCracken, H.M., 1979. Plate tectonics, *Earth Science Atlas,* Bureau of Mineral Resources, Canberra, Australia.

Shor, G.G., Jr., Kirk, H.K. & Menard, H.W., 1971. Crustal structure of the Melanesian area, *J. geophys. Res.,* **76,** 2562–2586.

Van der Hilst, R.D., Kennett, B.L.N., Christie, D. & Grant, J., 1994. Skippy: mobile broad-band arrays to study the seismic structure of the lithosphere and mantle beneath Australia, *EOS, Trans. Am. geophys. Un.,* **75,** 177–181.

Vidale, J.E., 1986. Complex polarization analysis of particle motion, *Bull. seism. Soc. Am.,* **76,** 1393–1405.

Zielhuis, A. & Van der Hilst, R.D., 1996. Upper-mantle shear velocity beneath eastern Australia from inversion of waveforms from SKIPPY portable arrays, *Geophys. J. Int.,* **127,** 1–16.